Journal of Hazardous Materials 178 (2010) 535–540

Contents lists available at ScienceDirect

Journal of Hazardous Materials

journal homepage: www.elsevier.com/locate/jhazmat

Influence of velocity gradient in a hydraulic flocculator on NOM removal by aerated spiral-wound ultrafiltration membranes (ASWUF)

J.C. Rojas[b], B. Moreno[a], G. Garralón[c], F. Plaza[c], J. Pérez[a], M.A. Gómez[a,*]

[a] Technologies for Water Management and Treatment Research Group, Department of Civil Engineering and Water Research Institute, University of Granada, Campus de Fuentenueva s/n, 18071 Granada, Spain
[b] Faculty of Engineering and Architecture, University of Pamplona, Colombia
[c] Research and Development Department, CADAGUA S.A. Gran Vía 45, 8, 48011 Bilbao, Spain

ARTICLE INFO

Article history:
Received 15 July 2009
Received in revised form 21 January 2010
Accepted 22 January 2010
Available online 1 February 2010

Keywords:
Transmembrane pressure
Velocity gradient
Hydraulic flocculation
NOM
Aerated spiral-wound ultrafiltration membranes (ASWUF)

ABSTRACT

A hydraulic coagulation–flocculation processes combined with aerated spiral-wound ultrafiltration membranes (ASWUF) was designed with the objective of improving natural organic matter (NOM) removal by ASWUF in the treatment of water for human consumption. The pilot-scale experimental system had capacity for treating 0.9 m^3/h. Dosage of Cl_3Fe as coagulant and hydraulic retention time (HRT) were calculated to generate microflocculation and different velocity gradients (G = 27, 47, 87 and 104 s^{-1}) were applied in the hydraulic flocculator. Operating alone, the ASWUF system achieved an NOM removal performance of 39% without problems of membrane clogging, although there was a significant correlation between effluent and influent quality. Application of microflocculation achieved considerable improvement in NOM removal, but values of $G \leq 87\ s^{-1}$ resulted in rapid clogging of the membrane due to flocs disintegration in the aerated membrane tank. Particle analysis revealed that the reduction of the velocity gradient had the effect of inclining the particle size distribution towards larger sizes, affecting both NOM removal capacity and membrane clogging. For $G = 104\ s^{-1}$ an NOM removal yield of 90% was reached, while transmembrane pressure (TMP) was stabilised as a result of the control of membrane clogging.

1. Introduction

Membrane technologies such as ultrafiltration offer an interesting alternative to disinfection of water for human consumption [1,2]. Based on a screening mechanism, such systems have a high capacity for the elimination of microorganisms, including virus [3], without the problems of resistance which occur in other systems of disinfection. Membrane technologies do not employ chemical oxidants in water treatment and therefore avoid the problem of generating by-products. At the same time, membrane technologies improve the physico-chemical characteristics of the water, particularly with regard to the presence of particulate matter and turbidity [3].

Given these advantages, membrane technologies may be regarded as suitable for drinking water production and offer a considerable simplification of the processes involved [2]. However, the systems present two major problems: on the one hand, the rapid clogging of the membrane, and on the other hand, the low capacity for removal of dissolved compounds and small colloids. Accordingly, they are not very effective at removing natural organic matter (NOM).

Experiments carried out by Rojas et al. [2] demonstrate that membrane systems are incapable of exceeding 42% removal of NOM and present a strong correlation between the quality of influent and the permeate. Similarly, de la Rubia et al. [4] observed low NOM removal in ultrafiltration membranes (500–1000 Da), while nanofiltration membranes (150–430 Da) achieved significantly better results.

The consequences of low effectiveness in NOM removal have a direct impact on different parameters of water quality such as colour, smell and taste [5]. Additionally, the presence of organic material in the permeate water may lead to the development of biofilms [6], which affect both the membrane permeate zone and the storage and distribution system, posing a risk for public health [6]. This leads to the need for more chlorine in post-chlorination, which in turn increases the risk of generating chlorination by-products after membrane treatment [7].

Membrane clogging causes a loss of permeability in the system with the consequent reduction of flux or increase of transmembrane pressure (TMP), depending on the mode of operation applied [8,9]. One of the factors which contributes significantly to the loss of permeability and to membrane clogging is NOM, especially the

* Corresponding author. Tel.: +34 958 246153; fax: +34 958 246138.
E-mail address: mgomezn@ugr.es (M.A. Gómez).

0304-3894/$ – see front matter © 2010 Elsevier B.V. All rights reserved.
doi:10.1016/j.jhazmat.2010.01.116

presence of humic acids [5]. Similarly, researchers such as Jermann et al. [10] have observed that the main problems of load loss and reduction in membrane permeability are caused by colloidal particles, while Thorsen [8] determined that particles between 0.1 and 1.5 μm are chiefly responsible for critical membrane fouling.

To avoid problems deriving from membrane clogging, phases of backwashing may be alternated with short production times [11]. Alternatively, air or water may be applied over the surface of the membrane in order to prevent biofouling and other processes [12]. These alternatives have given rise to a considerable diversity of membrane configurations and operational characteristics, in the search for increased production and greater competitiveness.

A further technique to improve NOM removal yields is to use membranes with a reduced molecular weight cut-off [4]. However, this type of membrane presents greater problems of permeability loss and clogging. On the other hand, application of coagulation–flocculation as pretreatment to microfiltration and ultrafiltration has proved to be highly efficient at increasing virus removal capacity [13]. Additionally, this technique may improve elimination of organic material in ultrafiltration and, according to authors such as Xia et al. [14] and Chen et al. [15], may even reduce problems of clogging in ultrafiltration membranes. However, other authors such as Carroll et al. [16] have found that the coagulation process increases problems of load loss and membrane clogging.

The flocculation process requires particular attention, since the application of a specific velocity gradient (G) and hydraulic retention time (HRT) determines the production of different types of flocs which may be more or less easy to eliminate by physical processes. Flocculation presents certain limitations when applied prior to membrane aeration, since the aeration tends to disintegrate the flocs and thus render the process inefficient. In sum, the processes of coagulation–flocculation–ultrafiltration need to be configured very carefully to optimize the system, and to guarantee the viability of NOM elimination by means of these technologies.

One of the most widespread membrane configurations in water treatment is the spiral-wound membrane, which is highly robust and offers a large membrane surface area. Ultrafiltration membranes of this type have proved efficient for potabilization [2]. In order to reduce the frequency of backwashing and chemical cleaning, the system is often operated with a constant airflow (aerated spiral-wound ultrafiltration or ASWUF), which reduces the accumulation of particles on the membrane surface. However, as mentioned above, this limits the application of flocculation.

With these considerations in mind, a hydraulic vertical flow flocculator was designed with the aim of generating a microflocculation that would permit the successful combination of ASWUF membranes with coagulation–flocculation. This system has certain advantages such as simplicity of operation and maintenance, due to the absence of mechanical elements and external energy demands. By means of the hydraulic flocculator, different velocity gradients were applied under a constant hydraulic retention time and coagulation dose, in order to create microflocs. In this way, it was possible to evaluate the impact of the velocity gradient (G) on the efficiency of an ASWUF membrane applied to groundwater potabilization.

2. Materials and methods

2.1. Experimental pilot installation

The experiment was carried out using a pilot-scale plant which operated constantly throughout the experimental process, thereby simulating a real situation with progressive fouling of the membrane. Water used in the experiment was sourced from the *Canales* reservoir in the province of Granada, Spain. Original characteristics of the water were not modified.

The experimental plant was composed of the following components (Fig. 1):

- Injection pump with a capacity for 1 m^3/h, 3 bar, providing a constant influent of 0.9 m^3/h.
- Ring-filter macrofiltration pretreatment phase (150 μm).
- In-line mixer with injection port for coagulant dosage, with a mixer length of 12″.
- Vertical hydraulic flocculation tank with a volume of 100 L (HRT = 6.6 min). Water was distributed by means of three perforated distribution lines equipped with manually operated closure valves. The system featured a differential pressure gauge to calculate the applied velocity gradient.
- Aerated ultrafiltration module equipped with spiral-wound (ASWUF) polyethersulphone membranes (TriSep Corporation), with an effective pore size of 0.05 μm, installed in a 150 L capacity tank. The area of filtration was 16.6 m^2 (flux = 54 L/m^2 h), operating in a vacuum with a TMP of −0.2 bar. Working conditions consisted of production periods of 60 min (0.9 m^3/h) with continuous aeration (12 Nm^3/h), followed by backwashing phases of 2 min (2 m^3/h), using filtered water. Chemical cleaning was carried out daily with chlorine (100 mg/L, pH = 11), and once a week using citric acid (250 mg/L, pH = 4.5).

2.2. Experimental procedure

The experimental pilot plant operated continuously in automatic mode. Backwashing was activated for set periods and by means of a continuous TMP monitor which activated backwashing periods at values superior to −0.6 bar. A fan provided continuous air supply over the membrane (12 m^3/h, 1.18 bar) during the production phase. Permeate water was used for backwashing. Chemical cleaning phases were activated automatically on a time basis and manually depending on the TMP registered after backwashing. Chemical cleaning consisted of six steps: tank drainage, tank fill with chemical solution, static soaking cycle (0.4 h), recirculation (1.0 h), tank drainage, and backwashing.

The system operated for a period of one month without coagulation or flocculation. Thereafter a constant coagulation dose was applied, together with an HRT in the flocculator of 6.6 min. The differential pressure in the flocculator was varied to obtain different velocity gradients (G = 27, 47, 87 and 104 s^{-1}). Duration of each phase was dependent on the efficiency of the process on the basis of TMP.

2.3. Coagulant dose determination

Various low HRTs were tested for the microflocculation process and an ideal coagulant dose was selected for the generation of small stable flocs in the membrane tank.

To determine the ideal coagulant dose, a Jar Test was carried out using Cl_3Fe. In this process, progressively larger doses of coagulant (from 0.2 to 8.0 mg/L) were added to 1 L of influent. The reactive was added for 30 s at 150 rpm and for 6.6 min with slow stirring, after which the water was passed through 0.22 μm filters. Analyses were then carried out for turbidity, pH, permanganate oxidability and residual iron. This test was repeated applying different slow stirring values (10, 20, 30, 40 and 50 rpm). Finally, optical microscopy was used to study the size of the largest flocs generated, which did not exceed 100 μm.

By means of this test an optimum dose of 4 mg Cl_3Fe/L was determined. This quantity was the minimum dose for which lowest values of turbidity and permanganate oxidability were obtained, after passing the sample through filters of 0.22 μm. Values for pH and residual iron concentration were within established lim-

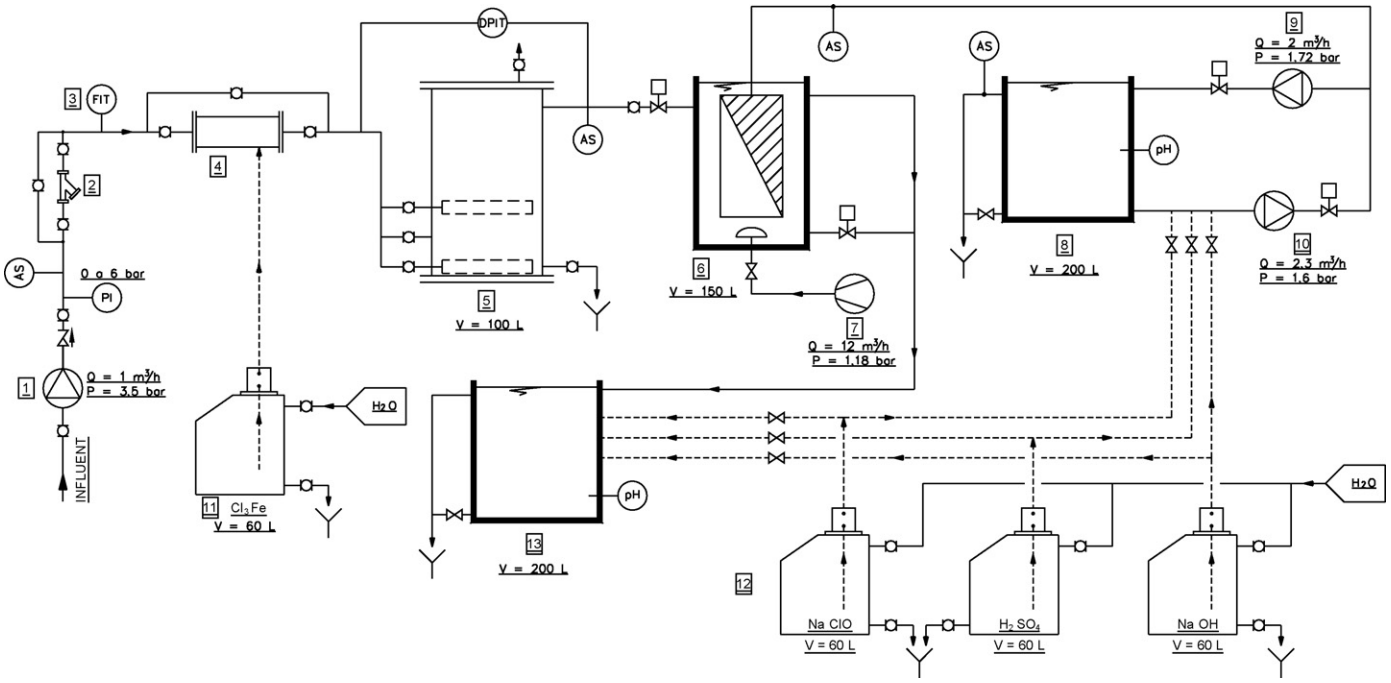

Fig. 1. Schematic diagram of experimental pilot plant. Influent pump (1), screen (2), flow indicator and transmitter (3), in line mixer (4), hydraulic flocculation tank (5), membrane module (6), fan (7), permeate tank (8), permeate pump (9), backwashing pump (10), Cl_3Fe dosage (11), chemical cleaning dosage (12), and rejet neutralization tank (13). AS: analytical sampler; PI: pressure indicator; DPIT: differential pressure indicator and transmitter.

its for water destined for human consumption (Council Directive 98/83/EEC).

2.4. Analytical methods

For physico-chemical analysis, water samples were collected daily in thoroughly cleansed plastic bottles and analysed immediately. Analytic determination of turbidity was carried out using the quantitative diffuse radiation method described in Regulation UNE-EN ISO 7027:2001. Determination of permanganate oxidability was based on the method described in Regulation UNE-EN ISO 846:1995. For the determination of $UV_{254\,nm}$ absorbance, an UV–visible spectrophotometer was used (Heλios γ). Suspended solids concentration was established by a filtration method using 0.45 μm filters, as reflected in *Standard methods for the examination of water and wastewater* [17]. For colour determination, the technique described in Regulation UNE-EN ISO 7887:1995 was used. For bacteriological and viral analyses, water samples were collected in sterile glass bottles (1 L) and analysed immediately after collection. The presence of *Escherichia coli* was studied using the membrane filtration procedure (UNE-EN ISO 9308-1:2001). Somatic coliphages were examined using a modified form of the double agar layer method of Adams described by Rojas et al. [2].

Particle size distribution (PSD) was conducted using a LiQuilaz-E20 particle counter (Particle Measuring Systems), in which the measuring principle is based on laser light extinction, calibrated by inert latex particles of defined size. A volume of 10 mL set at a fixed rate was analysed for each sample. Parallel to this, size of flocs in the membrane tank was analysed using optical microscopy (Motic) with 4× and 10× objectives. A graduated ocular micrometer was employed, calibrated by means of a 1.0 mm segment stage micrometer with graduation up to 10 μm.

2.5. Statistical analysis

All data obtained in this study were analysed using the statistical program STAGRAPHICS Plus 3.0 for Windows. For each assay, absorbance values at 254 nm and permanganate oxidability values in the influent were compared with those of the effluent, and the corresponding linear correlation coefficients were obtained in each case.

The different particle distributions in the samples after the flocculation process were subject to a mathematical adjustment, according to which the value of the integration of the regression obtained from the coordinate axes between the value of the smallest particle analysed and the maximum size recorded ($y = 0$)

Table 1
Influent characteristics and removal yields (%) for each assayed configuration with the ASWUF system.

Parameter	Influent characteristics	Without C–F	With C–F			
			$27\ s^{-1}$	$47\ s^{-1}$	$87\ s^{-1}$	$104\ s^{-1}$
Turbidity	4.57 NTU	96.1 ± 5.1	94.6 ± 9.3	95.2 ± 7.8	94.8 ± 9.3	97.1 ± 4.2
TSS	5.3 mg/L	100	100	100	100	100
$Colour_{436\,nm}$	0.21 m^{-1}	99.9 ± 1.1	100	100	100	100
MnO_4^- Ox	1.01 mg O_2/L	38.8 ± 4.5	75.2 ± 1.5	75.7 ± 1.75	78.6 ± 2.1	89.2 ± 2.6
UVA_{254}	1.65 m^{-1}	37.7 ± 6.7	37.9 ± 5.6	51.1 ± 5.7	52.5 ± 4.6	59.1 ± 4.6
E. coli	2801 cfu/100 mL	100	100	100	100	100
Somatic coliphages	51 pfu/100 mL	100	100	100	100	100

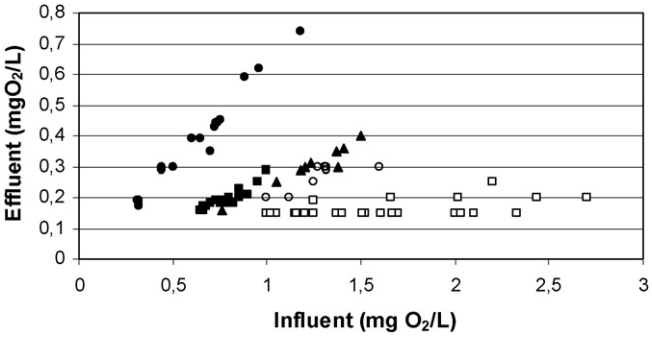

Fig. 2. Influent and effluent MnO_4^- oxidability correlation without coagulation–flocculation (●) and with flocculation at different velocity gradients: $G = 27\ s^{-1}$ (■), $G = 47\ s^{-1}$ (▲), $G = 87\ s^{-1}$ (○), and $G = 104\ s^{-1}$ (□).

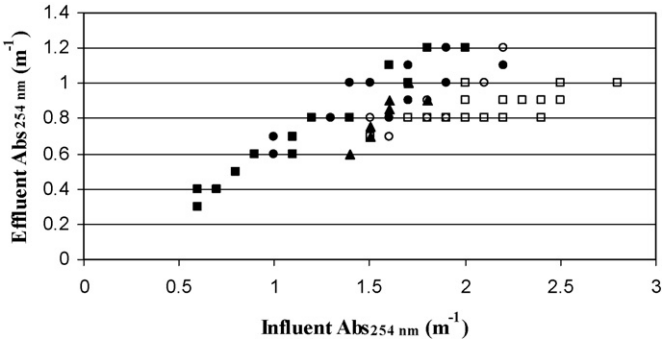

Fig. 3. Influent and effluent $Ab_{254\,nm}$ correlation without coagulation–flocculation (●) and with flocculation at different velocity gradients: $G = 27\ s^{-1}$ (■), $G = 47\ s^{-1}$ (▲), $G = 87\ s^{-1}$ (○), and $G = 104\ s^{-1}$ (□).

was calculated. These values were compared for each completed test.

3. Results and discussion

Table 1 shows the characteristics of the influent and the yields (%) of the ASWUF system for water potabilization, with and without previous flocculation. As may be seen, the membrane is highly efficient at removing virus and bacteria, achieving a total absence in all the measurements carried out. Given that the average pore size of the membrane (0.05 μm) is similar to the size of virus such as coliphages, a considerable removal capacity was to be expected. However, many of these infectious elements succeed in passing through ultrafiltration membranes, owing to the variability of pore size with respect to the nominal size [13]. In a continuous operating system, the screening process results in the formation of cake on the membrane surface due to the accumulation of retained material, and this has been observed to enhance the viral removal capacity of membrane technologies [18]. These factors, together with the low presence of coliphages in the influent (≈50 pfu/100 mL), explain their total absence in the permeate, rendering it unnecessary to apply the coagulation–flocculation process in order to improve this parameter.

Other physico-chemical parameters such as turbidity, suspended solids concentration and colour also presented a considerable improvement, owing to the membrane's capacity for retaining particulate matter. Membrane efficiency at controlling these parameters without the need for previous coagulation–flocculation has been demonstrated in previous research [2]. Indeed, the presence of particles is often due to the progressive fouling of the permeate zone rather than their ability to pass through the membrane [3].

The most critical aspect of ultrafiltration systems applied to water potablization is the elimination of NOM. This is composed of substances of different molecular weight; in reservoir water, compounds of between 1 and 100 kDa may be present [19]. In the present study, the influent presented an average organic material concentration of 1 mg O_2/L (MnO_4^- Ox), indicating a low concentration. For this influent, the application of a spiral-wound membrane with a molecular weight cut-off (MWCO) of 50 kDa was sufficient to achieve an average removal yield of 38.8% for organic material (Table 1). A high correlation was shown to exist between the concentration in the influent and the effluent, with a coefficient of determination $r^2 = 0.996$ (Fig. 2). This performance is significant bearing in mind the performance of conventional types of treatment such as those analysed by Wong et al. [19] (prechlorination–coagulation–flocculation–sedimentation–filtration–final disinfection), which did not exceed 16% for influents with similar concentrations of organic material.

A removal yield of 37.7% was also achieved for $UVA_{254\,nm}$ (Table 1), and again a high correlation was observed between the influent and effluent, with a coefficient of determination $r^2 = 0.870$ (Fig. 3). The application of this type of membrane is effective at retaining organic matter with highest molecular weight, such as humic acids, while the fraction of lowest weight, which may include humic substances such as fulvic acids [20], passes through the membrane.

In the experimental system, coagulation–flocculation processes were carried out in the membrane tank feed pipe, thus maintaining the pressure in the circuit. By means of a coagulant dosage with a concentration of 4 mg/L and subsequent hydraulic flocculation with an HRT of 6.6 min, it was possible to aggregate the small colloidal compounds in order to form microflocs, whose size was dependent on the velocity gradient applied. In a full-scale flocculation system, Bache and Rasool [21] studied the average size variation of flocs generated on the basis of velocity gradient and found that the largest size corresponded to $G \approx 33\ g^{-1}$, while for higher values the average floc size descended, with flocs of 100 μm for $G = 413\ s^{-1}$. The four different velocity gradients values assayed in the present experiment were: $G = 27, 47, 87$ and $104\ s^{-1}$. Optic microscopy confirmed that these differences affected floc size, which increased in line with the decrease in velocity gradient, with the largest flocs fluctuating between 45 and 100 μm.

It was anticipated that the size of the microflocs would be affected by the constant aeration applied in the membrane tank to combat rapid clogging. However, optical microscopy revealed the presence of flocs of similar size to those in the influent after the hydraulic flocculation, thus confirming the suitability of microflocculation for the ASWUF system. By contrast, a process of flocculation which generated large flocs would not have proved efficient, since the large flocs would be disintegrated by the aeration.

The results in Table 1 show a considerable increase in NOM removal yields after coagulation–flocculation and confirm that in spite of aeration in the membrane tank, NOM removal was influenced by variation in the hydraulic flocculator velocity gradient. The increase was evident in both MnO_4^- Ox and UVA_{254}, although there were differences in the removal values obtained and in their evolution. Figs. 2 and 3 show the relation between influent and effluent characteristics for each configuration assayed. As may be observed, the correlation declined as the velocity gradient increased. For determination of MnO_4^- Ox, values evolved from $r^2 = 0.8381$ for $G = 27\ s^{-1}$ to $r^2 = 0.2709$ for $G = 104\ s^{-1}$. A similar pattern was shown for UVA_{254} (Fig. 3), indicating that humic substances were predominant in the composition of the NOM influent.

Although the experimental ASWUF system operated with a constant flux of 54 L/m^2 h, variations in TMP occurred as a

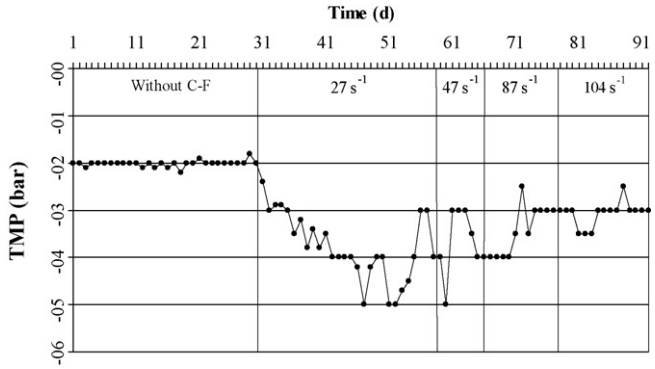

Fig. 4. Transmembrane pressure variation in spiral-wound membrane in function of applied velocity gradient.

consequence of membrane clogging. During the phase without coagulation–flocculation, TMP remained constant at −0.2 bar (Fig. 4) an optimum value for this membrane. In this phase, the frequency and duration of established backwashing cycles and chemical cleaning were sufficient to maintain TMP. However, once coagulation–flocculation was applied, a considerable increase in TMP was observed, with values nearing the permitted maximum for the experimental ASWUF system (−0.6 bar). As a result, it was necessary to double the frequency of backwashing and chlorine chemical cleaning, whereas acid chemical cleaning was carried out daily. In spite of which the TMP continued to present problems. However, increasing the velocity gradient in the hydraulic flocculator proved more efficient than backwashing and chemical cleaning. Through this technique, it was possible to reduce TMP to appropriate values (Fig. 4) and to revert to the established periodicity for backwashing and chemical cleaning when G was 104 s^{-1}.

For systems operating with constant flux, membrane clogging results in an increase in TMP, and this was immediately apparent in the experimental system after applying coagulation–flocculation as pretreatment. Since the quality of the influent did not present any variation which might explain the increase in membrane clogging, it may be assumed that the origin of the problem was in the pretreatment.

Previous research has shown that a considerable decline in flux may arise in ultrafiltration processes owing to the blocking of membrane pores [8,9]. Park et al. [22] observed that membrane clogging indexes increased significantly in line with the decrease in the size of particles in the influent. According to Thorsen [8], the critical particle size for rapid membrane clogging in ultrafiltration and nanofiltration is in the range between 0.1 and 1.5 μm. Nevertheless, studies by Xia et al. [14] found that the application of coagulation as pretreatment to ultrafiltration membranes improved not only the quality of the permeate, but also the membrane flux for a constant TMP. According to these authors, the generation of flocs from colloids present in the water enhances membrane retention capacity at the same time as it generates a film which may be easily eliminated through backwashing. The formation of this floc-based film means that the small particles do not come into direct contact with the membrane, as a result of which membrane clogging is reduced.

In the present case, the fact that the application of coagulation–flocculation exacerbated membrane clogging may have been due to the aeration in the membrane tank, which would cause the fragmentation of the flocs generated through the hydraulic flocculation and thus increase the presence of small-sized particles. However, variations in the hydraulic flocculator velocity gradient affected the TMP in such a way that increasing the velocity gradient brought about a reduction in clogging, in spite of the constant aeration. In view of this, it is important to evaluate the distribution of particles in the influent after the hydraulic flocculation in order to estimate their effect on clogging.

Fig. 5 shows average distributions of particles between 2 and 80 μm in the coagulation–flocculation influent and in the effluent under the impact of different velocity gradients in the hydraulic flocculator. Comparison of the particle distribution in the influent and effluent clearly demonstrates the capacity of the system for retaining particulate material, with the best results achieved when the system is operating with a value of G = 104 s^{-1}. This result corroborates the superior quality of permeate water obtained using this configuration.

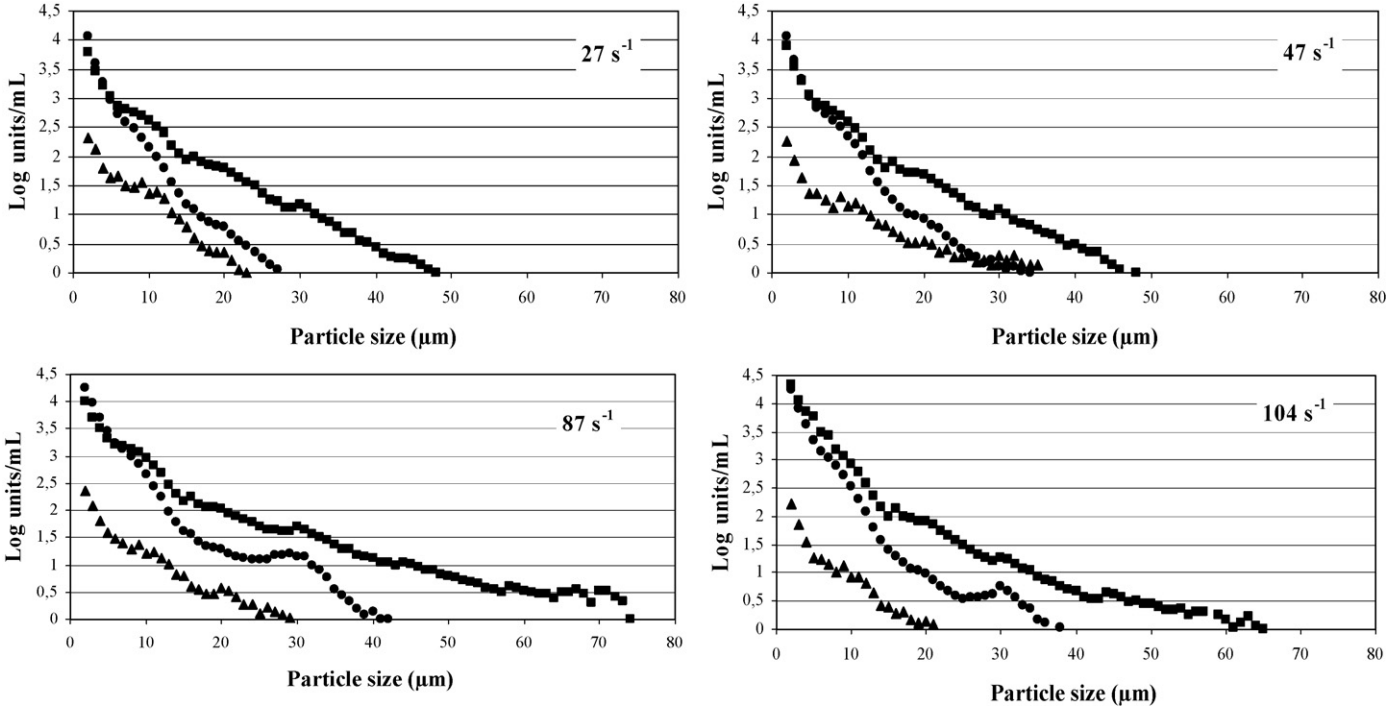

Fig. 5. Particle size distribution from 2 to 125 μm at different velocity gradients: influent (●), influent after coagulation–flocculation (■), and end effluent (▲).

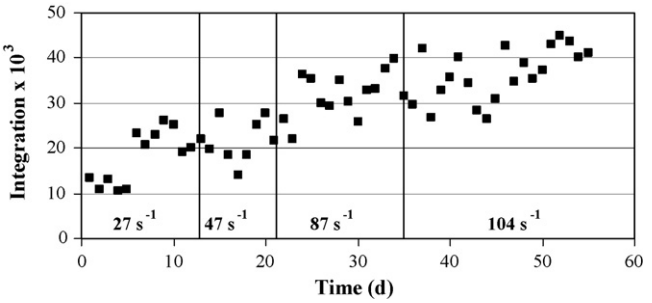

Fig. 6. Mathematical integration of logarithmic X-model regression from particle size distributions for influent after coagulation–flocculation.

Fig. 5 also shows average particle size distribution after hydraulic flocculation. In general, the distribution of small-sized particles (2–5 μm) remains similar to that observed in the influent, with the exception of tests carried out at $G = 104\,s^{-1}$, in which the number of small-sized particles increases. With regard to larger-sized particles (>10 μm), a significant increase in quantity is apparent for the different G values tested due to the applied microflocculation. Fig. 6 shows values obtained from the mathematical integration of the X-model regression for particle size distribution after hydraulic flocculation. As may be seen, values increase in line with the increase in G value. The ascending integration value is due to the progressive increase in the total number of particles between 2 and 80 μm. This in turn implies a reduction in the number of particles under 2 μm in size, due to the aggregation process.

If the distribution of particles in a water sample is considered typically presents a Gauss bell pattern, the aggregation of small-sized particles as an effect of the microflocculation brings about a shift in the particle distribution, in such a way that the maximum particle count inclines towards higher values in accordance with the increase in the velocity gradient applied. For G values under $87\,s^{-1}$, aggregation of colloids through microflocculation gave rise to the formation of particles with a negative effect on the permeability of the membrane, causing it to block. According to Thorsen [8], the presence in water of particles between 0.1 and 1.5 μm is directly related to membrane clogging. Particles of this size tend to be drawn towards the membrane in the production process, blocking the pores and generating a relatively hard and compact cake which is difficult to eliminate through backwashing. However, increasing the G value to $104\,s^{-1}$ caused the particle distribution curve to shift towards a larger size for maximum count flocs, meaning that the resulting cake was less compact while direct blockage of the membrane pores was avoided. All these factors made it possible to maintain an adequate flux and achieve better control over the loss of permeability through backwashing, as has been found in other studies concerning the application of coagulation–flocculation as a pretreatment to membrane filtration [14,15].

4. Conclusions

The main drawback in the application of ultrafiltration for drinking water production is the low efficiency of the system at retaining NOM, particularly compounds of low molecular weight, so that effluent quality depends on the quality of the influent. An alternative for improving performance in this respect is to incorporate a coagulation–flocculation process as pretreatment to membrane filtration. However, this process has proved to be inefficient when using aerated spiral-wound membranes (ASWUF), owing to the disintegration of the flocs caused by the aeration employed to prevent rapid membrane clogging. A possible solution is to apply microflocculation through hydraulic flocculation, using a low hydraulic retention time and a low dose of coagulant. This has the effect of producing small flocs which remain relatively stable when exposed to the aeration process. This method brings about a considerable increase in NOM removal capacity, but it has the major drawback of causing rapid membrane clogging due to the small-sized flocs. However, a suitable adjustment of the velocity gradient applied in the hydraulic flocculation can create an optimum floc size, permitting an improvement in NOM removal yields without exacerbating problems of membrane clogging. Using this technique, the combination of coagulation–microflocculation processes with ASWUF is a technically viable option achieving high efficiency in the removal of NOM from water destined for human consumption.

Acknowledgements

This study was supported by funds of the European Union and the Spanish Ministry of Education and Science (CIT-310200-2005-22). It was conducted at the Institute of Water Research with the collaboration of CADAGUA S.A. and EMASAGRA S.A. The article was translated from Spanish by Julian Bourne of the Faculty of Translation and Interpreting, University of Granada.

References

[1] J.M. Laine, D. Vial, P. Moulart, Status after 10 years of operation—overview of UF technology, Desalination 131 (2000) 17–25.
[2] J.C. Rojas, B. Moreno, G. Garralón, F. Plaza, J.I. Pérez, M.A. Gómez, Potabilization of low NOM reservoir water by ultrafiltration spiral wound membranes, J. Hazard. Mater. 158 (2008) 593–598.
[3] M. Gómez, A. de la Rua, G. Garralón, F. Plaza, E. Hontoria, M.A. Gómez, Urban wastewater disinfection by filtration technologies, Desalination 190 (2006) 16–28.
[4] A. de la Rubia, M. Rodríguez, V.M. León, D. Prats, Removal of natural organic matter and THM formation potential by ultra and nanofiltration of surface water, Water Res. 42 (2008) 714–722.
[5] E. Aoustin, A.I. Schäfer, A.G. Fane, T.D. Waite, Ultrafiltration of natural organic matter, Sep. Purif. Technol. 22–23 (2001) 63–78.
[6] S.L. Percival, J.T. Walter, P.R. Hunter, Microbiological Aspects of Biofilm and Drinking Water, CRC Press, New York, 2000.
[7] R.C. Andrews, M.J. Ferguson, Minimizing disinfection by-products formation while ensuring Giardia control, in: R.A. Minear, G.L. Amy (Eds.), Disinfection By-products in Water Treatment, Lewis Publishers, New York, 2000.
[8] T. Thorsen, Concentration polarisation by natural organic matter (NOM) in NF and UF, J. Membr. Sci. 233 (2004) 79–91.
[9] H. Choi, H.S. Kim, I.T. Yeom, D.D. Dionysious, Pilot plant study of an ultrafiltration membrane system for drinking water treatment operated in the feed-and-bleed mode, Desalination 172 (2005) 281–291.
[10] D. Jermann, W. Pronk, S. Meylan, M. Boller, Interplay of different NOM fouling mechanisms during ultrafiltration for drinking water production, Water Res. 41 (2007) 1713–1722.
[11] P. Lipp, M. Witte, G. Baldauf, A.A. Povorov, Treatment of reservoir water with a backwashable MF/UF spiral wound membrane, Desalination 179 (2005) 83–94.
[12] E.R. Cornelissen, L. Rebour, D. van der Kooij, L.P. Wessels, Optimization of air/water cleaning (AWC) in spiral wound element, Desalination 236 (2009) 266–272.
[13] L. Fiksdal, T. Leiknes, The effect of coagulation with MF/UF membrane filtration for the removal of virus in drinking water, J. Membr. Sci. 279 (2006) 364–371.
[14] S. Xia, J. Nan, R. Lui, G. Li, Study of drinking water treatment by ultrafiltration of surface water and its application to China, Desalination 170 (2004) 41–47.
[15] Y. Chen, B.Z. Dong, N.Y. Gao, J.C. Fan, Effect of coagulation pretreatment on fouling of an ultrafiltration membrane, Desalination 204 (2007) 181–188.
[16] T. Carroll, S. King, S.R. Gray, B.A. Bolto, N.A. Booker, The fouling of microfiltration membranes by NOM after coagulation treatment, Water Res. 34 (2000) 2861–2868.
[17] APPHA, AWWA, WEF, Standard Methods for the Examination of Water and Wastewater, 18th ed., American Public Health Association, Washington, DC, 1992.
[18] S.S. Madaeni, A.G. Fane, G.S. Grohmann, Virus removal from water and wastewater using membranes, J. Membr. Sci. 102 (1995) 65–75.
[19] H. Wong, K.M. Mok, X.J. Fan, Natural organic matter and formation of trihalomethanes in two water treatment processes, Desalination 210 (2007) 44–51.
[20] Y.P. Chin, G. Alken, E. O'Loughlin, Molecular weight, polydispersity, and spectroscopic properties of aquatic humic substances, Environ. Sci. Technol. 28 (1994) 1853–1858.
[21] D.H. Bache, E. Rasool, Floc size distribution in a stirred suspension, Water Sci. Technol. 53 (2006) 103–112.
[22] C. Park, H. Kim, S. Hong, S. Choi, Variation and prediction of membrane fouling index under various feed water characteristics, J. Membr. Sci. 275 (2006) 29–36.